J. Biomater. Sci. Polymer Edn, Vol. 16, No. 12, pp. 1575–1593 (2005)

Also available online - www.vsppub.com

Chemical modification of chitosan by phosphorylation: an XPS, FT-IR and SEM study

I. F. AMARAL [1,2,*], P. L. GRANJA [1] and M. A. BARBOSA [1,2]

[1] *INEB — Instituto de Engenharia Biomédica, Laboratório de Biomateriais, Rua do Campo Alegre, 823, 4150-180 Porto, Portugal*
[2] *Universidade do Porto, Faculdade de Engenharia, Departamento de Engenharia Metalúrgica e de Materiais, Porto, Portugal*

Received 2 November 2004; accepted 31 May 2005

Abstract—In the present work, the surface of chitosan membranes was modified using a phosphorylation method carried out at room temperature. Phosphorylation may be of particular interest in materials for orthopaedic applications, due to the cation-exchange properties of phosphate functionalities. Phosphate groups chelate calcium ions, thus inducing the deposition of an apatite-like layer known to improve the osteoconduction of polymer-based implants. Additionally, the negatively charged phosphate functionalities, together with the positively charged amine groups from chitosan, are expected to provide chitosan with an amphoteric character, which may be useful as a combinatorial therapeutic strategy, by simultaneously allowing the immobilization of signalling molecules like growth factors. Phosphorylation was carried out at room temperature using the $H_3PO_4/Et_3PO_4/P_2O_5$/butanol method. Surface characterization was performed by XPS, ATR–FT-IR, and SEM. Cross-sections were analyzed by SEM fitted with EDS. The phosphate content increased with the reaction time, as shown by XPS and ATR–FT-IR, a P/N atomic ratio of 0.73 being obtained after 48 h of treatment. High-resolution XPS spectra regarding C_{1s}, O_{1s}, N_{1s} and P_{2p} are discussed. The introduction of a neutralization step led to a reduction of P content, which pointed out to the presence of phosphates ionically bound to protonated amines, in addition to phosphate esters. EDS analysis of cross-sections revealed a gradual P reduction up to 50% towards the inner part of the membrane.

Key words: Chitosan; phosphate; phosphorylation; X-ray photoelectron spectroscopy (XPS); Fourier transform infrared spectroscopy (FT-IR); SEM-EDS; surface chemical reaction.

INTRODUCTION

Chitosan is a linear co-polymer of glucosamine and *N*-acetyl glucosamine in a $\beta 1 \rightarrow 4$ linkage obtained by *N*-deacetylation of chitin. It is a biodegradable

*To whom correspondence should be addressed. Tel.: (351-22) 607-4982. Fax: (351-22) 609-4567. E-mail: iamaral@ineb.up.pt

polysaccharide with well-established biocompatibility, presently under investigation for a wide range of biomedical applications such as sutures, wound dressings, bone substitutes, tissue engineering and gene- and drug-delivery vehicles [1, 2].

In orthopaedics, its degradability associated to its structural similarity to extracellular matrix glycosaminoglycans makes it an attractive bio-polymer for bone tissue repair. However, despite leading to satisfactory results when applied to bone defects in animal models, namely increased osteogenesis and angiogenic activity without fibrous tissue invasion, chitosan is not sufficiently osteogenic to induce the desired rapid bone regeneration at the initial stage of bone healing [3, 4]. Hence, chitosan has been frequently associated with calcium phosphates, not only due to the well-established osteoconduction of calcium phosphates, but also based on its analogy to collagen, the organic matrix of bone on which the inorganic phase mineralizes [5, 6].

Phosphorylation of chitosan seems to be of particular interest for orthopaedic applications, due to the cation-exchange properties of phosphate functionalities. Phosphate groups bind calcium ions, which may then induce the formation of a calcium phosphate layer known to promote the osteoconduction of polymer-based implants [7]. Thus, coating chitosan membranes with a porous apatite-like layer is expected to improve cell attachment and migration, allowing its use as membranes for guided bone regeneration.

Phosphorylated chitosan membranes were reported to induce the biomimetic deposition of an apatite-like layer under simulated physiological conditions, after pre-incubation in calcium-containing solutions, due to chelation of calcium ions and partial hydrolysis of phosphate functionalities [8, 9].

The incorporation of phosphate functionalities on chitosan substrates could also be of interest for other biomedical applications like tissue engineering. Surface binding of signalling molecules onto resorbable scaffolds is a concept which is gaining increasing interest in regenerative medicine, in contrast to the use of diffusible growth factors [10]. Phosphate groups, due to their ion-exchange properties, constitute adequate functionalities for specifically binding biologically active species [11, 12]. Phosphate carriers are cation exchangers, based on their ability to exchange ionically bound cations (e.g., Na^+, Ca^{2+}) with cationic residues of biomolecules in solution. Phosphorylation of porous chitosan matrices can be used to immobilize signalling biomolecules, such as growth factors promoting tissue regeneration. The ionic character of these chemical bindings, together with the mild conditions for immobilization used, usually leads to minor conformational changes of the immobilized biomolecule with subsequent retention of activity [13].

Phosphorylated chitosan membranes may also be of interest for the culture of certain anchorage-dependent cells. Cell attachment to chitosan is mainly attributed to electrostatic interactions between the chitosan cationic sites, provided by protonated amine groups from glucosamine units, and the negatively charged carboxylate and sulphate groups found in cell-surface proteoglycans [14]. However, strong attachment to chitosan substrates may hinder cell spreading and migration, as reported for fibroblasts [14]. Hence, the grafting of anionic groups on chitosan

can be useful to tailor surface charge, thus balancing strong electrostatic interactions affecting cell behaviour.

Phosphorylation of cellulose under mild conditions has recently been reported [15]. This method has the advantages of leading to highly substituted products, as well as of being carried out at room temperature, resulting in low degradation of the polymer. Additionally, it has been shown to provide *in vitro* cytocompatibility and *in vivo* integration in bone tissue [16]. However, the application of this chemical modification route to other polysaccharides has not been reported yet.

Phosphate esters of chitin and chitosan were initially prepared due to their metal-ion-binding capabilities and basically two preparation techniques were used. The first one is based on the synthesis route of cellulose phosphates, consisting of heating chitin/chitosan at high temperature (usually 150°C) with phosphoric acid and urea in dimethylformamide [17, 18]. The second method reported was developed by Nishi *et al*. [19], and involves the reaction of chitin/chitosan dissolved in methanesulphonic acid with phosphorus pentoxide at low temperature (0–5°C).

In the present work, the $H_3PO_4/Et_3PO_4/P_2O_5$/hexanol method [15] was applied to the phosphorylation of squid chitosan membranes for different time periods. The amount of covalently bound phosphates introduced through this phosphorylation method has been estimated. Surface characterization was performed using complementary spectroscopic techniques, namely X-ray photoelectron spectroscopy (XPS) and Fourier transform infrared spectroscopy with attenuated total reflectance (ATR–FT-IR). Cross-sections of the modified membranes were also observed by scanning electron microscopy (SEM), fitted with an energy dispersive X-ray analysis system (EDS), in order to evaluate the extent of phosphorylation along the membrane thickness.

MATERIALS AND METHODS

Materials

Chitosan powder from squid pens was kindly donated by France Chitine (France). All reagents used were of analytical grade.

Purification of chitosan

Chitosan was purified by the reprecipitation method. Briefly, chitosan was dissolved in 3% (v/v) aqueous acetic acid overnight and, after complete dissolution, the resulting gel was filtered through a No. 1 sintered glass funnel, to remove undissolved or gelatinous particles. Chitosan was then precipitated through the dropwise addition of 1 M aqueous NaOH, while stirring. Finally, the regenerated chitosan was thoroughly washed with distilled and dionized water (DDW) until neutrality, freeze-dried and grounded in a laboratory mill to yield a fine powder (40–75 μm).

Characterization of chitosan

Chitosan was characterized in terms of *N*-acetylation degree and average molecular weight. The degree of *N*-acetylation (DA) was determined by FT-IR spectroscopy, using the KBr technique. Each pellet was prepared by blending 2 mg purified chitosan powder, previously dried overnight at 60°C under reduced pressure, with 100 mg KBr, previously dried at 105°C for 24 h. The infrared spectra were immediately recorded with a FT-IR system 2000 from Perkin-Elmer, by accumulation of 200 interferograms, at a 4 cm^{-1} spectral resolution. The amide-I band ($\nu = 1655$ cm^{-1}) was used as the analytical band and the hydroxyl band ($\nu = 3450$ cm^{-1}) as the internal reference band. The DA was calculated according to the method proposed by Baxter *et al*. [20], as follows:

$$\mathrm{DA}(\%) = (A_{1655}/A_{3450}) \times 115. \tag{1}$$

Average molecular weight was determined by viscometry, in a solvent system of 0.1 M CH_3COONa/0.2 M CH_3COOH. Flow times of sample solutions were measured immediately, to avoid chain depolymerization, using an Ubbelohde viscometer 0c (Shott Geräte) at 30 ± 0.1°C, with an automated viscosity measuring system (Lauda mgw) and an extra temperature controller (Comarck). Intrinsic viscosity ($[\eta]$) was obtained from linear plots of reduced viscosity (η_{sp}/C) against concentration (C), extrapolating to zero concentration. Viscosity average molecular weight (M_v) was calculated based on the Mark–Houwink equation, as follows:

$$[\eta] = K M_v^a, \tag{2}$$

where, according to chitosans in this system, $K = 1.64 \times 10^{-30} \times \mathrm{DD}^{14}$ and $a = -1.02 \times 10^{-2} \times \mathrm{DD} + 1.82$ [21]; DD is the degree of *N*-deacetylation (%) of chitosan, which is the inverse of the DA.

Preparation of chitosan membranes

Membranes were prepared by solvent casting, from 1% (w/v) solutions of purified chitosan in 1% (v/v) aqueous acetic acid. After complete dissolution, the resulting gel was filtered, kept under reduced pressure in order to clear all the entrapped gas bubbles and poured into 120×120 mm^2 polystyrene petri dishes (60 g per plate). The gel was allowed to settle for 48 h at room temperature in a laminar flow hood. The resulting membranes were deprotonated in 0.5 M aqueous NaOH for 1 h and thoroughly washed with DDW. Finally, they were cut into 30×60 mm^2 strips, and kept in absolute ethanol prior to chemical modification. For characterization purposes, chitosan membranes were dried at 30°C for 24 h in a vacuum oven, and stored in a desiccator until further analysis. Membrane thickness was measured with a Mitutoyo dial thickness gauge No. 7301.

Acetylation of chitosan

Chitosan membranes were acetylated at room temperature [22, 23]. The membranes were steeped in an aqueous methanolic acetic acid solution (water/methanol/acetic acid = 50 : 200 : 1, v/v) and acetic anhydride (5.0 mol per glucosamine residue) was added. After 12 h under stirring the membranes were rinsed in methanol, followed by rinsing in ethanol, and then steeped in 0.5 M ethanolic KOH overnight to remove any ester groups. The membranes were finally washed with ethanol, followed by DDW, and then dried at 30°C for 24 h in a vacuum oven. The corresponding degree of *N*-acetylation was estimated according to Shigemasa *et al.* [24], using the amide-II band ($\nu = 1560\ cm^{-1}$) as the analytical band and the C−O stretching band ($\nu = 1070\ cm^{-1}$) as the internal reference band. In ATR–FT-IR spectra, the internal reference band at 3450 cm^{-1}, previously used for determining the DA of chitosan powder, presents low absorbance values when compared to transmission spectra.

Phosphorylation of chitosan

Surface phosphorylation was performed using the $H_3PO_4/Et_3PO_4/P_2O_5$/hexanol method [15], substituting hexanol by 2-butanol, which has a higher water solubility. Briefly, 1 g chitosan membrane strips was suspended in 40 ml 2-butanol in a round-bottomed flask. The reaction mixture was prepared by adding 43 ml H_3PO_4 to 37 ml Et_3PO_4, followed by step-by-step addition of P_2O_5 under constant stirring. The resulting translucent solution was then gradually added to the flask. The reaction was allowed to proceed under N_2 atmosphere at 30°C, with constant stirring in a thermostatised orbital shaker. Phosphorylation was carried out for different time periods, up to 48 h. After chemical treatment, membranes were rinsed with ethanol and suspended twice in this solvent for 30 min. Finally, they were dialyzed against DDW for 24 h to remove free inorganic phosphate, and dried at 30°C for 24 h in a vacuum oven. Acetylated chitosan membranes, in which amines are absent, were also phosphorylated for a period of 8 h. Alternatively, acetylated and original chitosan membranes which were phosphorylated for 8 h were both subjected to neutralization after the ethanol rinsing step. The neutralization step was used in order to convert chitosan ammonium groups into uncharged amine groups, with consequent release of ionically bound phosphates. The strips were incubated in 0.5 M aqueous NaOH at 25°C for 30 min under stirring, thoroughly washed with DDW until neutral pH, and finally dialyzed and dried as previously described.

Surface characterization

X-ray photoelectron spectroscopy (XPS). Spectra were obtained on a VG Scientific ESCALAB 200 A, using Mg Kα X-ray radiation as the excitation source (15 kV), operated at 300 W. The analyzer was run in the constant analyzer trans-

mission mode. The emitted photoelectrons were analyzed at a 90° take-off angle from the horizontal surface plane, for all analysis. Survey spectra were acquired over a binding energy range of 0 to 1100 eV, using a pass energy of 50 eV. High-resolution spectra for the C_{1s}, O_{1s}, N_{1s} and P_{2p} regions were obtained, using a pass energy of 20 eV. Due to their insulating nature, chitosan membrane surfaces became positively charged after the emission of photoelectrons, resulting in a broadening of the spectral lines and a drift toward higher binding energy [25]. Thus, the binding energies of the photoelectron peaks were calibrated, assigning a binding energy of 285.0 eV to the aliphatic carbon ($-CH_2-$) C_{1s} peak, present as a carbon surface contaminant [25]. The deconvolution of the high resolution spectra was made by means of a least-squares peak analysis software, XPSPEAK version 4.1, using the Gaussian/Lorenzian sum function. A linear background was used for carbon and phosphorous regions, while an integral background based on the Shirley method was used for the oxygen and nitrogen regions [26]. Initial assumptions on the possible species were derived from chitosan stoichiometry and chemical bonds. Element atomic percentages were calculated from the integrated intensities of the XPS peaks, taking into account the atomic sensitivity factors of the instrument data system.

Fourier transform infrared spectroscopy with attenuated total reflectance (ATR–FT-IR). The infrared spectra were recorded with a FT-IR system 2000 from Perkin-Elmer, using the SplitPea™ accessory (Harrick Scientific), provided with a silicon internal reflection element and configured for external reflectance mode. The membranes were previously dried at 60°C in a vacuum oven for 12 h. The spectra were obtained from a 200 μm diameter sampling area, after accumulation of 200 interferograms, at a 4 cm^{-1} spectral resolution. All spectra were corrected for the ATR characteristic progressive increase in the absorbance at lower wave numbers, using the equipment software. Peak identification was obtained from the correspondent second-derivative spectra in the range between 1250 and 800 cm^{-1}, where the characteristic vibrations from phosphates were expected to occur.

Scanning electron microscopy (SEM) with energy-dispersive X-ray analysis (EDS). Observation was performed using a Jeol JSM-6301F scanning electron microscope, equipped with a Noran-Voyager energy dispersive spectroscope. In order to obtain a brittle fracture, the membranes were cryofractured in liquid N_2, followed by drying under vacuum. For SEM, the samples were gold sputtered and observed at an accelerating voltage of 5 kV, in order to avoid membrane degradation. For EDS analysis, samples were carbon sputtered and the correspondent cross-sections were analyzed at an accelerating voltage of 10 kV. EDS quantification of phosphorous/carbon intensity ratio was normalized to 100% at the surface, for each sample.

RESULTS AND DISCUSSION

Characterization of chitosan

Regenerated chitosan presented a DA of 39% (molar fraction of *N*-acetylated units = 0.39), and an average viscosity molecular mass of 2480 kDa, which is in the range of the molecular masses reported for squid chitosan [27].

The membranes obtained were clear and transparent, with a smooth shiny surface, in accordance with reports using the same chitosan animal source [28]. The membranes were flexible, presenting an average film thickness of 53 ± 3 μm.

After acetylation, the ATR–FT-IR spectra of chitosan membranes revealed the absence of the peak at 3360 cm^{-1}, assigned to the NH_2 asymmetric stretching, suggesting full acetylation of chitosan amine groups. In accordance, a DA of *ca.* 100% was found.

Preparation and characterization of phosphorylated chitosan membranes

Physical appearance. During reaction, chitosan membranes retained their original form and did not stick to each other. After drying, the modified membranes seemed similar to unmodified membranes, at the macroscopic level, being transparent and flexible.

X-ray photoelectron spectroscopy (XPS). The survey spectra of chitosan membranes confirmed the presence of carbon, oxygen and nitrogen. After phosphorylation, phosphorus was easily detected on all membranes, irrespective of the reaction time used. The possible phosphorylated products are illustrated in Fig. 1. Both primary and secondary chitosan hydroxyl groups, namely at the C-6 and C-3 positions of the glucosamine units, are likely to be esterified by phosphorylation. In a recent work, Wang *et al.* [29] reported a preferential substitution of the hydroxyl group at the C-6 position, for low degrees of substitution. Due to the acidic nature of the reaction medium, chitosan amine groups were ionized, and thus probably involved in ionic bindings with free phosphate ions ($H_2PO_4^-$ and HPO_4^{2-}) (product a) [30]. In addition, since chitosan has a considerable amount of amine groups, inter or intrachain ionic bonds — salt linkages — between phosphate groups and protonated amine groups are likely to be formed (product b) [19]. The formation of pyrophosphates from condensation of phosphates in chitosan chains, together with condensation of phosphates with incoming phosphoric acid from the reaction media, may also occur (product c) [30]. Lee and co-workers [30] suggested the formation of pyrophosphates and polyphosphates when chitosan membranes were reacted with orthophosphoric acid and urea. However, when the present method was applied to cellulose, pyrophosphates were not found [15].

Regarding element atomic percentages, chitosan membranes revealed more carbon and less oxygen and nitrogen, when compared to the expected values for chitosan presenting a DA of 39%, which may be due to carbon surface contamination

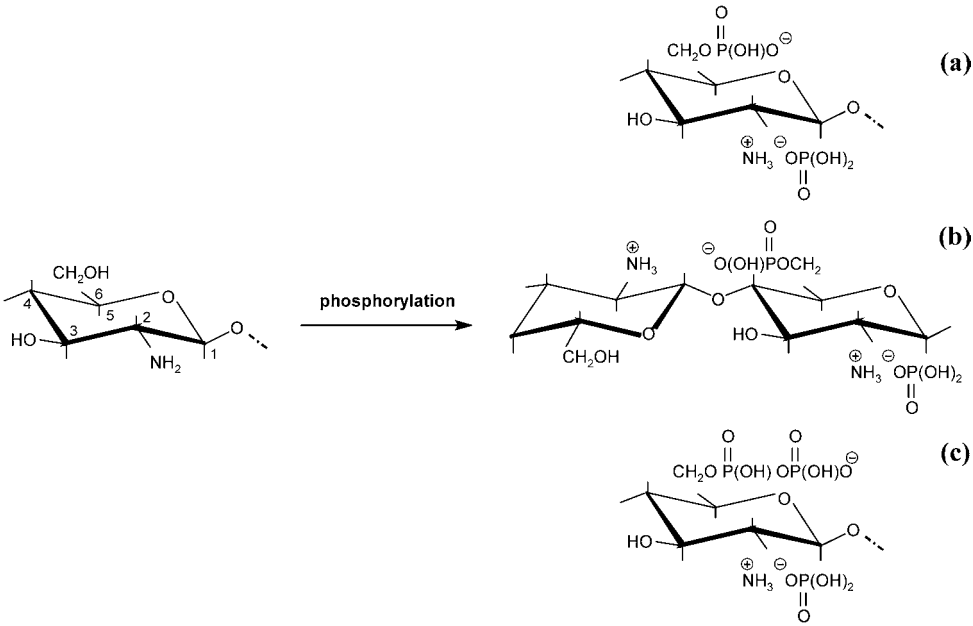

Figure 1. Chemical structure of possible phosphorylation products, in which chitosan amine groups are probably involved in ionic bindings with free phosphate ions, $H_2PO_4^-$ or HPO_4^{2-}. (a) Chitosan phosphate, esterified at the hydroxyl group at the C-6 position; (b) formation of inter- or intra-chain ionic bonds between chitosan phosphate groups and protonated amine groups from adjacent chitosan chains; (c) formation of pyrophosphates from condensation of phosphates in chitosan chains, together with condensation of phosphates with incoming phosphoric acid from the reaction media.

Table 1.
XPS element analysis (at%) as a function of phosphorylation reaction time

Reaction time (h)	C_{1s}	O_{1s}	N_{1s}	P_{2p}
0	62.2 (60.9; 64.1)	31.2 (29.2; 32.4)	7.08 (6.49; 7.79)	0.00
1	60.7 (59.3; 62.0)	31.6 (30.0; 33.0)	6.71 (6.61; 6.81)	1.06 (1.04; 1.08)
4	56.3 (55.0; 57.7)	35.0 (34.0; 36.3)	6.42 (6.22; 6.53)	2.31 (2.11; 2.50)
8	53.8 (53.3; 54.1)	36.5 (36.3; 36.8)	6.84 (6.65; 6.99)	2.87 (2.73; 2.99)
12	53.3 (52.5; 54.4)	37.0 (35.9; 37.5)	6.80 (6.73; 6.90)	2.96 (2.86; 3.08)
24	52.0 (50.8; 53.1)	37.9 (37.0; 38.7)	6.68 (6.48; 6.98)	3.42 (3.34; 3.49)
48	52.3 (51.4; 53.2)	36.5 (35.9; 37.1)	6.50 (6.37; 6.64)	4.71 (4.54; 4.89)

Results presented are the average (min; max) of three independent measurements.

(Table 1). Nevertheless, when the O/N atomic ratio of unmodified chitosan was calculated, a value of 4.41 was found, which is close to the expected one (4.39). The phosphorus atomic percentage increased logarithmically with reaction time, from approximately 1.0 to 4.7, as the membrane was reacted from 1 to 48 h. If expressed as a function of nitrogen, a P/N atomic ratio of 0.73 was obtained after 48 h (Fig. 2), which can be correlated to the degree of substitution at the surface, given that one

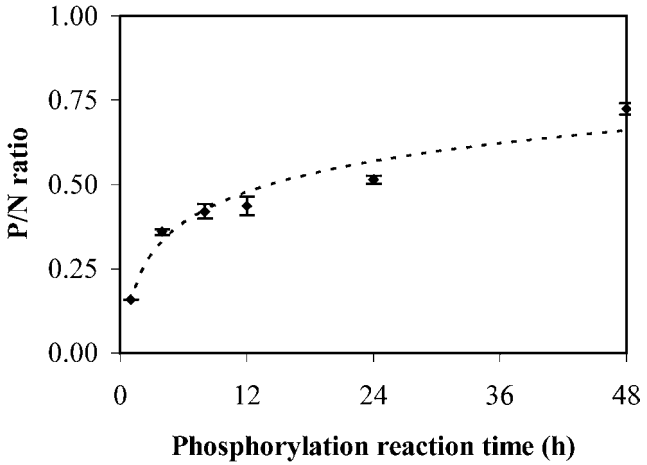

Figure 2. P/N ratio (at%) determined by XPS, as a function of phosphorylation reaction time.

nitrogen atom is present in each chitosan monomeric unit. Phosphorylation was more effective in terms of grafted phosphate groups during the first 4 h, becoming less effective after this period, probably due to the consumption of reactive hydroxyl groups. In addition, as a result of increasing reaction time, simultaneous hydrolysis of phosphate esters may have occurred, as reported for cellulose phosphates [15]. The oxygen amount also increased with reaction time, as expected. For each grafted phosphate group, three new oxygen atoms are introduced. The observed O/P ratios were plotted against reaction time and compared to the expected values calculated using equation (3) by normalizing the element surface concentrations to nitrogen content (Fig. 3).

$$\mathrm{O/P} = \frac{4.39 + (3 \times \mathrm{P/N})}{\mathrm{P/N}}, \tag{3}$$

where 4.39 is the O/N atomic ratio in unmodified chitosan membranes.

As shown in Fig. 3, the O/P ratios are in agreement with the expected values, for all reaction times experimented.

The effect of NaOH treatment is presented in Table 2. As previously stated, NaOH treatment was carried out to in order to convert positively charged chitosan ammonium groups into uncharged amines. The NaOH neutralization step led to a decrease of surface phosphorus amount in the range of 50%, for the 8 h phosphorylated chitosan membranes, which was attributed to the release of phosphate ions ionically bound to protonated amines. Pyrophosphates, if present, were possibly hydrolyzed upon NaOH treatment, contributing to the reduction of the amount of P [31]. The remaining phosphorus probably corresponds to the covalently bound phosphates (chitosan phosphate esters), as phosphate monoesters of polysaccharides were shown to be remarkably stable to base-catalyzed hydrolysis [32]. The alkaline stability of phosphate esters has been known for a long time, and explained as being due to electrostatic repulsion by the phosphate dianion and the base hydroxyl anion [32]. For

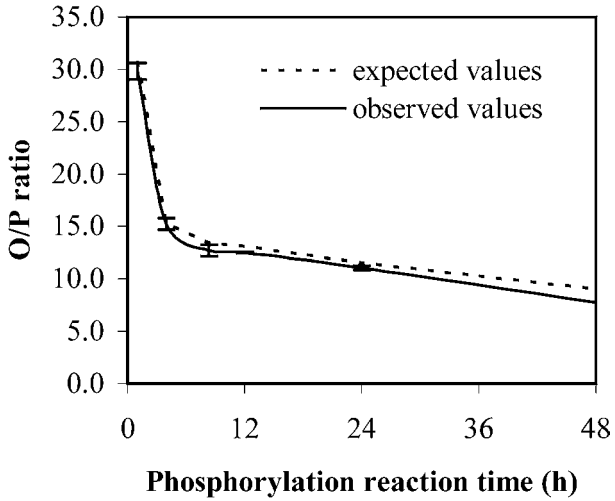

Figure 3. O/P ratio (at%) determined by XPS, as a function of phosphorylation reaction time.

Table 2.
XPS phosphorus (at%) of unmodified and fully acetylated chitosan membranes after an 8 h phosphorylation treatment, with or without subsequent neutralization in 0.5 M aqueous NaOH

	Unmodified chitosan (DA = 39%)	Acetylated chitosan (DA = 100%)
P-chitosan	2.79	1.17
NaOH-treated P-chitosan	1.46	1.08

DA, degree of *N*-acetylation of chitosan; P-chitosan, phosphorylated chitosan.

the same phosphorylation period, acetylated membranes revealed a lower surface phosphorus amount, namely of 1.17. In acetylated membranes, hydrogen bonding is stronger than in chitosan membranes, resulting in less hydroxyl groups available for phosphorylation [33]. After the NaOH treatment, an almost complete retention of P amount was observed, as expected. Acetyl groups, in contrast to amino groups, remain uncharged during phosphorylation. As a result, incorporation of phosphates through ionic binding with positively charged amines is not possible. It is worth mentioning that ionically bound phosphates were equally present, in an uncertain amount, when the phosphorylation of chitosan membranes by the phosphoric acid/urea/DMF method was reported [30].

The peak deconvolution of the high resolution spectra provided the chemical composition of the membranes at the surface, as indicated below.

C_{1s} spectra. The resolved C_{1s} spectrum regarding chitosan membranes revealed three peaks (figure not shown). The C_{1s} peak at 285.0 eV was mainly assigned to the carbon surface contaminant $-\underline{C}H_2-$, but also to $\underline{C}-NH_2$ chemical bindings, given that amines are reported to induce small chemical shifts, namely of 0.6 eV [34]. The peak at 286.6 eV was assigned to $\underline{C}-O$, $\underline{C}-OH$ and $\underline{C}-N-C=O$ and the peak

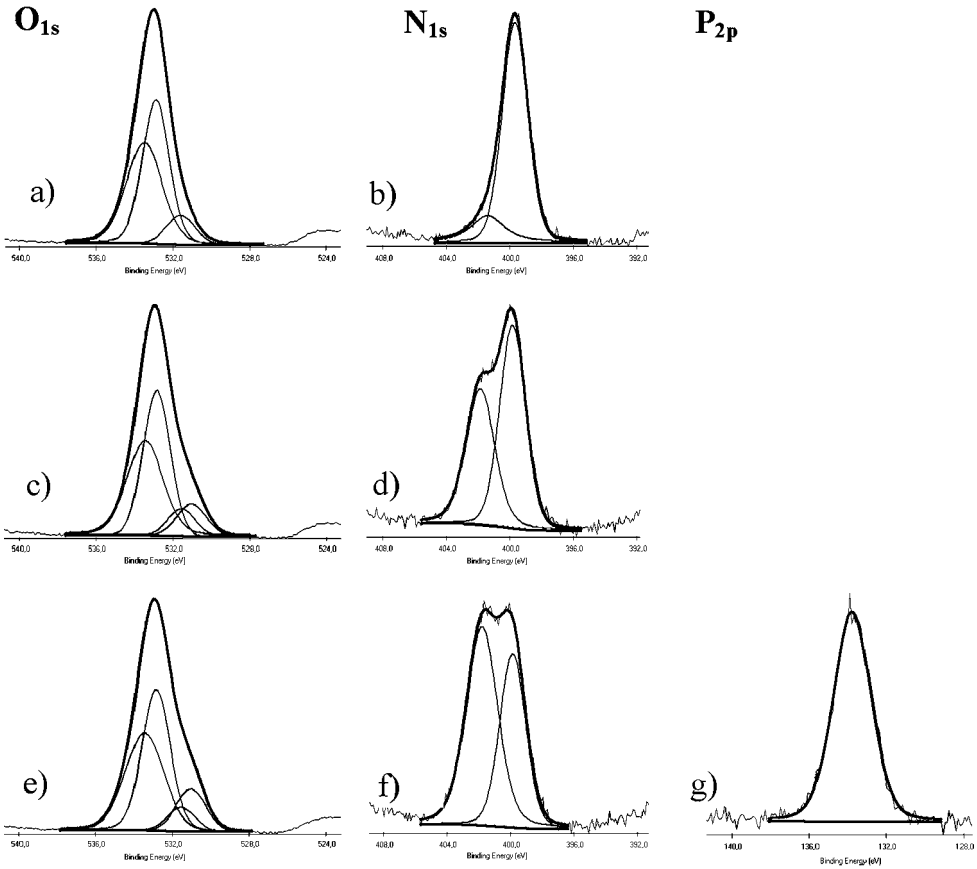

Figure 4. XPS high resolution spectra of: (a, b) unmodified chitosan membrane; (c, d) 8 h phosphorylated chitosan membrane; (e–g) 48 h phosphorylated chitosan membrane. O_{1s}, N_{1s} and P_{2p} regions are shown. The P_{2p} spectra of 8 h phosphorylated chitosan membrane is not shown, since the spectrum obtained was similar to that of the membranes phosphorylated for 48 h.

at 288.3 eV to O−C−O and N−C=O chemical bindings [34–36]. Spectra from phosphorylated samples did not reveal significant changes, regardless of the reaction time. The C_{1s} peak correspondent to C−O−P chemical bindings, expected to be centred at 286.4 eV [35, 37], was probably overlapped by chitosan C−OH chemical bindings, observed at 286.6 eV.

O_{1s} spectra. O_{1s} levels are rather broad in nature (2.0 eV). In addition, only few works are available concerning deconvolution of O_{1s} region of phosphate esters, to allow a reliable data interpretation [37]. Nevertheless, the results of the fit assumptions are summarized in Fig. 4. Regarding the spectrum of unmodified chitosan membranes (Fig. 4a), three peaks were identified. The peak at 531.6 eV was assigned to N−C=O chemical bindings in *N*-acetylated-glucosamine units [33, 35]. The peaks at 532.9 eV and 533.5 eV were assigned to C−OH and O−C−O chemical bindings, respectively [35]. Spectra from phosphorylated

samples presented a new peak at 531.0 eV (Fig. 4c and e), the intensity of which increased with reaction time (Table 3). This peak was assigned to physisorbed water, possibly associated with the presence of phosphorous functionalities [38], as well as to HPO_4^{2-} groups, ionically bound to protonated amine groups [39, 40]. According to Nishi and co-workers [19], phosphate esters present two pK_a values for the phosphate group, namely pK_{a1}, approx. 3.7, and pK_{a2}, approx. 8.5. Thus, at the pH of distilled water (approx. 5.3) phosphate functionalities should be in the form of monohydrogen phosphates ($-HPO_4^-$). The O_{1s} peaks corresponding to these groups and to $H_2PO_4^-$ ionic species are expected to be centred at 531.8 eV [40, 41] and were probably overlapped by chitosan chemical bindings. In addition, the peaks regarding oxygen atoms from C−O−P chemical bindings, reported to be centred at 533.5 eV in phosphate esters, could not be observed, probably due to overlapping by chitosan O−C−O chemical bindings, observed at 533.5 eV [37]. NaOH treatment led to a decrease of the intensity of the O_{1s} component centred at 531.0 eV (previously assigned to HPO_4^{2-} ionic species and to physisorbed water associated with phosphates), in agreement with the lower phosphorus amount observed, after the release of ionically bound phosphates (figure not shown).

N_{1s} spectra. The resolved N_{1s} spectra of chitosan membranes are shown in Fig. 4b. Two peaks were identified. The peak at 399.7 eV was assigned to N−C=O and NH_2 chemical bindings [40], while the peak at 401.4 eV was assigned to amino groups in the ammonium form (NH_3^+) [42]. Both forms, NH_2 and NH_3^+, were likely to be present in chitosan membranes, taking into account the pK_a of chitosan amine groups (*ca.* 6.5) [43], and the fact that chitosan membranes were immersed in distilled water before being dried. Phosphorylation led to an increased number of nitrogen atoms in the ammonium form and, simultaneously, to a decrease of the intensity of the N_{1s} component centred at 399.8 eV (Fig. 4d and f), assigned to N−C=O and NH_2 chemical bindings, possibly due to the acidic nature of the reaction medium. After 48 h treatment, the N_{1s} component at 399.8 eV was reduced to 42% of total nitrogen peak intensity (Table 3), meaning that the nitrogen atoms that contributed to this peak were essentially from *N*-acetylated chitosan units (DA 39%). The upward shift of the electron binding energy of the peak assigned to NH_3^+ groups to 401.8 eV suggests the presence of protonated amines in the form of ammonium salts [37] as it was expected from ionic bindings, either with free phosphates or with phosphate groups in chitosan chains. After NaOH treatment, the intensity of the peak assigned to NH_3^+ groups was reduced, if compared to

Table 3.
XPS component intensity ratios of O_{1s} and N_{1s}, as a function of phosphorylation reaction time

Reaction time (h)	O_{1s} (531.0 eV)/O_{1s}	N_{1s} (NH−C=O, NH_2)/N_{1s}
0	—	0.84±0.03
8	0.09±0.01	0.56±0.01
48	0.14±0.01	0.42±0.01

the non-treated membranes, as expected (figure not shown). Nevertheless, this same peak was centred at 401.6 eV, a higher electron binding energy compared to the correspondent one in chitosan membranes, which suggests the presence of salt linkages established between protonated amine groups and phosphate groups in chitosan.

P_{2p} spectra. All spectra from phosphorylated samples revealed a single peak centred at 133.8 eV (Fig. 4g). The correspondent full-width at half-maximum (FWHM) is wide (2.3 eV), as is usual in the case of P_{2p}, since the resulting line observed corresponds to $P_{2p1/2}$ and $P_{2p3/2}$ core-line doublets. This peak was assigned to phosphate species and may arise from two contributions: (a) from $H_2PO_4^-$ and HPO_4^{2-} ionic species [39, 40]; and (b) from $-HPO_4^-$ groups in chitosan. In a similar work, cellulose phosphates presented a single P_{2p} peak at 133.7 eV, as well [44]. The NaOH treatment of phosphorylated membranes did not affect the electron binding energy of P_{2p} peak. In terms of reaction yield, it is difficult to compare the present method to the H_3PO_4/urea/DMF reaction system, the most widely used for the phosphorylation of chitosan matrices [8, 9, 30]. The amounts of phosphorus reported here were determined on surfaces and thus cannot be compared to those obtained through other phosphorylation routes, in which XPS studies were not performed [9, 30].

ATR–FT-IR spectroscopy. The ATR–FT-IR spectra of unmodified and phosphorylated chitosan membranes as a function of reaction time are shown in Fig. 5. ATR–FT-IR spectra of unmodified and of 48 h phosphorylated chitosan membranes are presented in Fig. 6, in a narrower spectral range (1250–800 cm^{-1}). The major spectral peaks observed in this range, as well as the correspondent peak assignments are shown in Table 4.

The spectrum of unmodified chitosan membranes showed characteristic peaks of amide I at 1650 cm^{-1} (C=O stretching), amide II at 1558 cm^{-1} (N−H in plane deformation coupled with C−N stretching), amide III (C−N stretching coupled with NH in plane deformation) and CH_2 wagging coupled with OH in plane deformation at 1317 cm^{-1} [45, 46]. The broad peak observed at 3200–3450 cm^{-1} has the contribution of different vibrations, namely the hydrogen-bonded OH stretching at 3426 cm^{-1}, the NH_2 asymmetric stretching at 3360 cm^{-1} and the NH stretching in interchain NH$\cdots$O=C bonding at 3293 cm^{-1} [45, 47]. The other peaks at 2873 cm^{-1} and 1375 cm^{-1} were assigned to CH stretching and CH_3 symmetric deformation, respectively [45, 46].

Phosphorylation led to an emerging shoulder at 1220 cm^{-1}, which can be attributed to the P=O asymmetric stretching from phosphates, as it is found in polynucleotides between 1200 and 1230 cm^{-1} [48]. Similar results were reported for phosphorylated chitin [17, 19]. An increase in the absorbance of the peak at 1064 cm^{-1} was also observed, and was assigned to the C−O−P stretching in phosphate esters, overlapping the C−O stretching vibrations in chitosan ether groups, in accordance to the substitution of an hydroxyl group by a phosphate

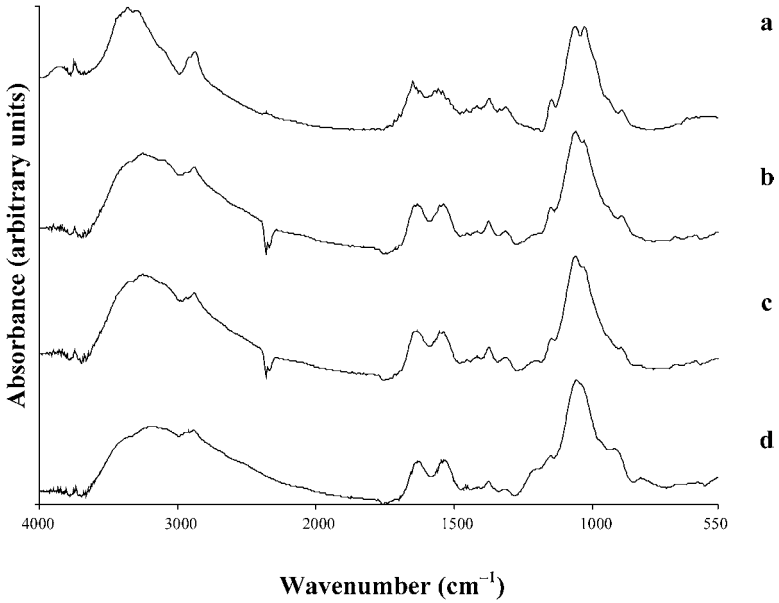

Figure 5. ATR–FT-IR spectra of (a) unmodified chitosan membrane; and chitosan membranes phosphorylated for (b) 4 h, (c) 24 h and (d) 48 h.

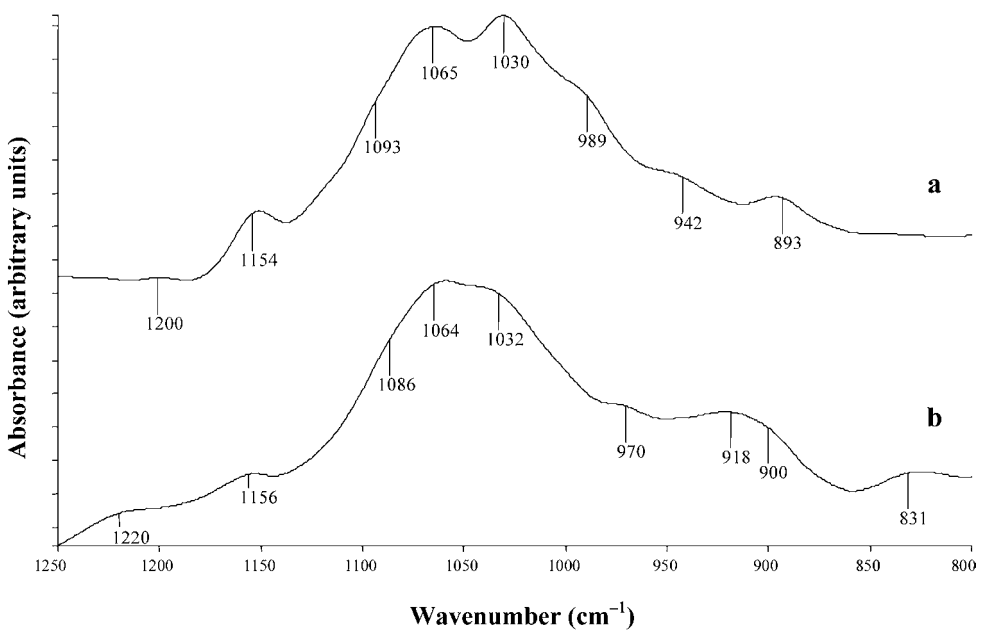

Figure 6. ATR–FT-IR spectra (1250–800 cm^{-1}) of (a) unmodified chitosan membrane and (b) 48 h phosphorylated chitosan membrane.

Table 4.
ATR–FT-IR spectra peak assignments of unmodified and 48 h phosphorylated chitosan membranes

Peak frequency (cm^{-1})		Peak assignment	Ref.
Chitosan	48 h P-chitosan		
—	1220	P=O asymmetric stretching	[17, 19, 48]
1200	—	Amine rocking	[45]
1154	1156	Asymmetric bridge oxygen stretching	[46]
1065	1064	−C−O stretching in ether groups	[24, 46]
		C−O−P stretching in phosphate esters	[49]
1030	1032	−C−O stretching in ether groups	[24, 46]
989	—	CH_3 rocking	[45]
—	970	P−OH stretching	[50]
942	—	CH_3 rocking	[45]
—	918	P−OH stretching	[17, 19, 50]
893	900	C−O ring stretching	[46]
—	831	P−O stretching in phosphate monoesters	[51]

P-chitosan: phosphorylated chitosan.

one [49]. Furthermore, the peaks detectable in the second derivative spectra, namely at 970 and 918 cm^{-1}, overlapping those of chitosan itself, as well as the peak at 831 cm^{-1}, point out the presence of phosphate functionalities [17, 19, 50, 51]. The decrease in the absorbance of the peak at 1317 cm^{-1} also suggests phosphorylation of hydroxyl groups. Protonation of chitosan amine functionalities is suggested by the presence of two peaks, both attributed to NH_3^+ groups, namely the anti-symmetrical deformation at 1630 cm^{-1} and the symmetric deformation at 1533 cm^{-1} [46]. The initial amide-I and -II bands were possibly overlapped by these vibrations. Concerning the region between 3450 and 2800 cm^{-1}, only a smoothing of the spectra was observed, which can be associated with a decrease in cristallinity [44]. In fact, in the case of phosphoric acid monoesters, the hydrogen-bonded OH groups may not appear significantly different from other strongly hydrogen-bonded hydroxyl groups [51]. The characteristic peak near 1440 cm^{-1}, indicating the presence of ammonium phosphates, was not observed, regardless of the treatments used.

SEM/EDS. Unmodified, as well as phosphorylated chitosan membranes revealed a smooth and homogeneous film surface. In the present work blisters or bubbles were not observed after chemical treatment, as opposite to the reported in literature when the H_3PO_4/urea/DMF method was used for the same purpose [9].

The cross-section of chitosan membranes (DA = 39%) revealed layers of fibrils measuring 0.15–0.35 μm in diameter, clearly oriented parallel to the surface. While chitosan membranes prepared from fully deacetylated chitosan are known to present rough cross-sectional ultrastructures, in which fibrils are absent, complete *N*-acetylation of the former was reported to lead to the formation of disorderly arranged fibrils [52]. Therefore, the observed fibrils were associated to the

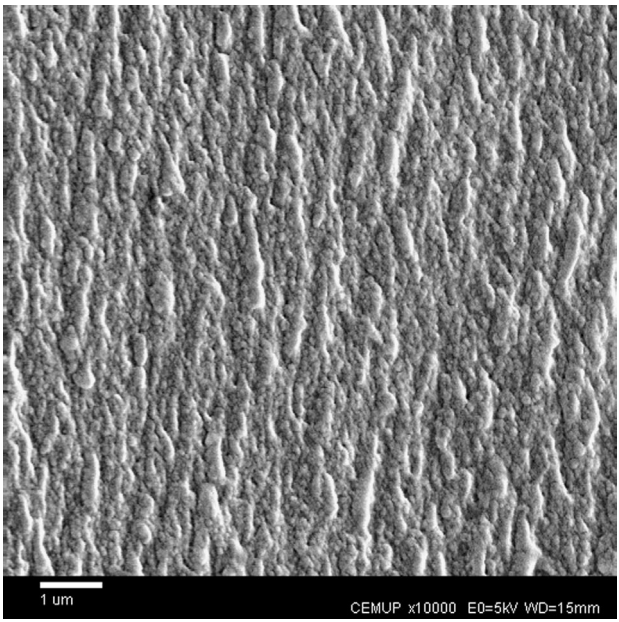

Figure 7. Scanning electron micrograph of the cross-section of N_2-fractured 8 h phosphorylated chitosan membrane.

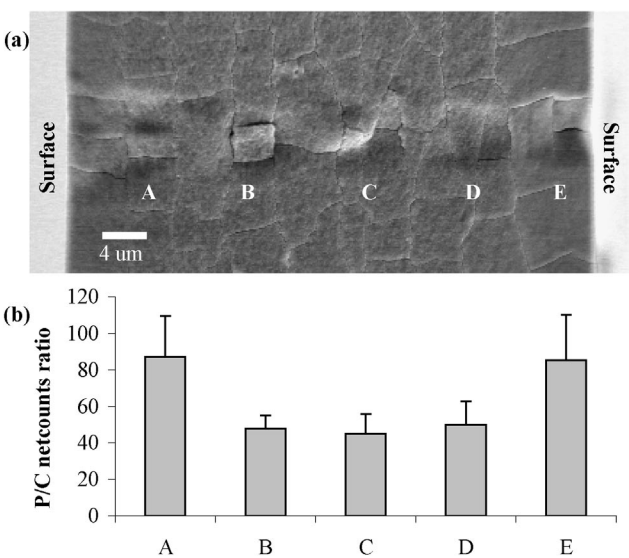

Figure 8. Profile of the P/C intensity ratio along the cross-section of a N_2-fractured 8 h phosphorylated chitosan membrane: (a) SEM image showing the areas (*ca.* 2×2 μm^2) where EDS analysis was performed (A–E); and (b) respective P/C intensity ratios. Intensity ratio was normalized to 100% at the surface ($n = 4$).

presence of partially *N*-acetylated chitosan chains, later compressed during the air-drying phase to form the membranes [52]. Figure 7 shows the cross-section of phosphorylated chitosan membranes, revealing essentially the same ultrastructure, regardless of the chemical treatment. Figure 8 shows the P/C intensity ratio profile along the cross-section of 8 h phosphorylated chitosan membranes, as determined by EDS. Analysis revealed higher levels of phosphorus at the surface, as expected, and a gradual P reduction up to 50% to the inner of the membrane.

CONCLUSIONS

Surface phosphorylation of chitosan membranes was achieved using the $H_3PO_4/Et_3PO_4/P_2O_5$/butanol reaction system, at room temperature. The surface phosphorous concentration increased with the reaction time, a maximum of 4.7 at% P being reached after 48 h of treatment. Phosphorylation also occurred in the inner of the membrane, although to a lower extent. Furthermore, phosphorylated membranes presented a considerably higher amount of ammonium ions ($-NH_3^+$) compared to unmodified membranes, as shown by XPS N_{1s} core level scan spectra. Chitosan-based surfaces carrying an amphoteric character were thus obtained, which may be used as a combinatorial strategy, to promote cell attachment and proliferation, while immobilizing signalling molecules. These materials can also be used to promote the deposition of an apatite-like layer on chitosan, to improve its osteoconduction.

Acknowledgements

This project was carried out under the contract PRAXIS/P/SAU/12288/1998. I. F. A. is grateful to the Portuguese Foundation for Science and Technology, for awarding her a scholarship under the PRAXIS XXI programme. Authors are grateful to France Chitine for the donation of the squid chitosan.

REFERENCES

1. E. Khor, *Chitin: Fulfilling a Biomaterials Promise*. Elsevier Science, Oxford (2001).
2. P. J. VandeVord, H. W. T. Matthew, S. P. DeSilva, L. Mayton, B. Wu and P. H. Wooley, *J. Biomed. Mater. Res.* **59**, 585 (2002).
3. R. A. A. Muzzarelli, M. Mattioli-Belmonte, C. Tietz, R. Biagini, G. Ferioli, M. A. Brunelli, M. Fini, R. Giardino, P. Ilari and G. Biagini, *Biomaterials* **15**, 1075 (1994).
4. J. Y. Lee, S. H. Nam, S. Y. Im, Y. J. Park, Y. M. Lee, Y. J. Seol, C. P. Chung and S. J. Lee, *J. Control. Rel.* **78**, 187 (2002).
5. R. A. A. Muzzarelli and C. Muzzarelli (Eds), in: *Chitosan in Pharmacy and Chemistry*, p. 233. Atec, Grottammare (2002).
6. F. Zhao, Y. J. Yin, W. W. Lu, J. C. Leong, W. J. Zhang, J. Y. Zhang, M. F. Zhang and K. D. Yao, *Biomaterials* **23**, 3227 (2002).
7. M. Tanahashi and T. Matsuda, *J. Biomed Mater. Res.* **34**, 305 (1997).
8. Y. Yokogawa, J. P. Reyes, M. R. Mucalo, M. Toriyama, Y. Kawamoto, T. Suzuki, K. Nishizawa, F. Nagata and T. Kamayama, *J. Mater. Sci. Mater. Med.* **8**, 407 (1997).

9. H. K. Varma, Y. Yokogawa, F. F. Espinosa, Y. Kawamoto, K. Nishizawa, F. Nagata and T. Kameyama, *Biomaterials* **20**, 879 (1999).
10. J. M. Orban, K. G. Marra and J. O. Hollinger, *Tissue Eng.* **8**, 529 (2002).
11. A. V. Ilyina, V. P. Varlamov, V. E. Tikhonov, I. A. Yamskov and V. A. Davankov, *Biotechnol. Appl. Biochem.* **19**, 199 (1994).
12. J. Sugihara, T. Imamura, T. Yanase, H. Yamada and T. Imoto, *J. Chromatogr.* **229**, 193 (1982).
13. J. F. Kennedy and J. M. S. Cabral, in: *Solid Phase Biochemistry: Analytical Synthetic Aspects*, W. H. Schouten (Ed.), p. 253. Wiley, New York, NY (1983).
14. C. Chatelet, O. Damour and A. Domard, *Biomaterials* **22**, 261 (2001).
15. P. L. Granja, L. Pouysegu, M. Petraud, B. De Jeso, C. Baquey and M. A. Barbosa, *J. Appl. Polym. Sci.* **82**, 3341 (2001).
16. J. C. Fricain, P. L. Granja, M. A. Barbosa, B. de Jeso, N. Barthe and C. Baquey, *Biomaterials* **23**, 971 (2002).
17. N. Sakairi, A. Shirai, S. Miyazaki, H. Tashiro, Y. Tsuji, H. Kawahara, T. Yoshida, N. Nishi and S. Tokura, *Kobunshi Ronbunshu* **55**, 212 (1998).
18. T. Sakaguchi, T. Horikoshi and A. Nakajima, *Agricult. Biol. Chem.* **45**, 2191 (1981).
19. N. Nishi, A. Ebina, S. Nishimura, A. Tsutsumi, O. Hasegawa and S. Tokura, *Int. J. Biol. Macromol.* **8**, 311 (1986).
20. A. Baxter, M. Dillon, K. D. A. Taylor and G. A. F. Roberts, *Int. J. Biol. Macromol.* **14**, 166 (1992).
21. W. Wang, S. Q. Bo, S. Q. Li and W. Qin, *Int. J. Biol. Macromol.* **13**, 281 (1991).
22. S. Aiba, *Int. J. Biol. Macromol.* **8**, 173 (1986).
23. S. Hirano, Y. Ohe and H. Ono, *Carbohydr. Res.* **47**, 315 (1976).
24. Y. Shigemasa, H. Matsuura, H. Sashiwa and H. Saimoto, *Int. J. Biol. Macromol.* **18**, 237 (1996).
25. M. P. Seah, in: *Practical Surface Analysis, Vol. 1*, D. Briggs and M. P. Seah (Eds), p. 541. Wiley, Chichester (1990).
26. P. M. A. Sherwood, in: *Practical Surface Analysis, Vol. 1*, D. Briggs and M. P. Seah (Eds), p. 555. Wiley, Chichester (1990).
27. S. M. Hudson and C. Smith, in: *Bio-polymers from Renewable Resources*, D. L. Kaplan (Ed.), p. 96. Springer, Berlin (1998).
28. R. Shepherd, S. Reader and A. Falshaw, *Glycoconj. J.* **14**, 535 (1997).
29. X. H. Wang, J. B. Ma, Y. N. Wang and B. L. He, *Biomaterials* **22**, 2247 (2001).
30. Y. M. Lee and E. M. Shin, *J. Membr. Sci.* **64**, 145 (1991).
31. S. S. Kim, W. Y. Jeong, B. C. Shin, S. Y. Oh, H. W. Kim and J. M. Rhee, *J. Biomed. Mater. Res.* **40**, 401 (1998).
32. R. L. Whistler and G. A. Towle, *Arch. Biochem. Biophys.* **135**, 396 (1969).
33. S. D. Gardner, C. S. K. Singamsetty, G. L. Booth and G. He, *Carbon* **33**, 587 (1995).
34. D. Briggs, in: *Practical Surface Analysis, Vol. 1*, D. Briggs and M. P. Seah (Eds), p. 437. Wiley, Chichester (1990).
35. G. D. B. Beamson, *High Resolution XPS of Organic Polymers*. Wiley, Chichester (1992).
36. B. D. Ratner and D. G. Caster, in: *Surface Analysis — The Principal Techniques*, J. C. Vickerman (Ed.), p. 43. Wiley, Chichester (1997).
37. S. Bourbigot, M. Lebras, L. Gengembre and R. Delobel, *Appl. Surf. Sci.* **81**, 299 (1994).
38. D. V. Kilpadi, G. N. Raikar, J. Liu, J. E. Lemons, Y. Vohra and J. C. Gregory, *J. Biomed. Mater. Res.* **40**, 646 (1998).
39. W. J. Landis, *J. Vac. Technol. A* **2**, 1108 (1984).
40. C. D. Wagner, A. V. Naumkin, A. Kraut-Vass, J. W. Alisson, C. J. Powell and J. R. Rumble, Jr., *NIST-X-ray Photoelectron Spectroscopy Database 20 Version 3.4*. National Institute of Standards and Technology, Gaithersburg, MD (2003). Available online at http://srdata.nist.gov/xps/
41. D. T. Quan, A. Le Bloa, H. Habib, O. Bonnaud, J. Meinnel, A. Quemerais and R. Marchand, *Rev. Phys. Appl.* **24**, 545 (1989).

42. B. Lindberg, R. Maripuu, K. Siegbahn, R. Larsson, C. G. Golander and J. C. Eriksson, *J. Colloid Interf. Sci.* **95**, 308 (1983).
43. A. Domard, in: *Advances in Chitin Science, Vol. 2*, A. Domard, G. Roberts and K. Vårum (Eds), p. 410. Jacques André, Lyon (1997).
44. P. L. Granja, L. Pouysegu, D. Deffieux, G. Daude, B. De Jeso, C. Labrugere, C. Baquey and M. A. Barbosa, *J. Appl. Polym. Sci.* **82**, 3354 (2001).
45. N. P. G. Roeges, *A Guide to the Complete Interpretation of Infrared Spectra of Organic Structures*. Wiley, Chichester (1994).
46. F. G. Pearson, R. H. Marchessault and C. Y. Liang, *J. Polym. Sci.* **43**, 101 (1960).
47. G. A. F. Roberts, *Chitin Chemistry*. Macmillan, London (1992).
48. A. H. Kuptsov and G. N. Zhizhin, *Handbook of Fourrier Transform Raman and Infrared Spectra of Polymers*. Elsevier, Amsterdam (1998).
49. L. W. Daasch and D. C. Smith, *Anal. Chem.* **23**, 854 (1951).
50. W. A. Bueno, *Manual de Espectroscopia Vibracional.* McGraw-Hill, São Paulo (1990).
51. R. A. Nyquist and C. D. Craver, *The Coblentz Society Desk Book of Infrared Spectra.* The Coblentz Society, French Village, MO (1977).
52. S. Hirano, K. Tobetto and Y. Noishiki, *J. Biomed. Mater. Res.* **15**, 903 (1981).